Neurobiology of Disease

Nicotine Blocks the Hyperpolarization-Activated Current I_h and Severely Impairs the Oscillatory Behavior of Oriens-Lacunosum Moleculare Interneurons

Marilena Griguoli,[1] Alena Maul,[1] Chuong Nguyen,[2] Alejandro Giorgetti,[3] Paolo Carloni,[2] and Enrico Cherubini[1]

[1]Neurobiology Department and Italian Institute of Technology Unit, International School for Advanced Studies (SISSA), 34014 Trieste, Italy, [2]Statistical and Biological Physics Department, SISSA, 34151 Trieste, Italy, and [3]Department of Biotechnology, University of Verona, 37134 Verona, Italy

In the brain, high cognitive functions are encoded by coherent network oscillations. Key players are inhibitory interneurons that, by releasing GABA into principal cells, pace targeted cells. Among these, oriens-lacunosum moleculare (O-LM) interneurons that provide a theta frequency patterned output to distal dendrites of pyramidal cells are endowed with HCN channels responsible for the slowly activating inwardly rectifying I_h current and their pacemaking activity. Here we show that, in transgenic mice expressing EGFP (enhanced green fluorescent protein) in a subset of stratum oriens somatostatin-containing interneurons that mostly comprise O-LM cells, nicotine, the active component of tobacco, reduced I_h and the oscillatory behavior of O-LM interneurons. In cells hyperpolarized at −90 mV, nicotine suppressed the theta resonance in the same way as ZD 7288 (4-ethylphenylamino-1,2-dimethyl-6-methylaminopyrimidinium chloride), a selective blocker of I_h. Nicotine blocked I_h in a concentration-dependent way with an EC_{50} of 62 nM. Similar effects were produced by epibatidine, a structural analog of nicotine. The effects of nicotine and epibatidine were independent on nicotinic ACh receptor (nAChR) activation because they persisted in the presence of nAChR antagonists. Furthermore, nicotine slowed down the interspike depolarizing slope and the firing rate, thus severely disrupting the oscillatory behavior of O-LM cells. Molecular modeling suggests that, similarly to ZD 7288, nicotine and epibatidine directly bind to the inner pore of the HCN channels. It is therefore likely that nicotine severely influences rhythmogenesis and high cognitive functions in smokers.

Introduction

The hippocampal network comprises a large variety of distinct locally connected GABAergic cells that exert a powerful control on network excitability and are responsible for the oscillatory behavior crucial for information processing in the brain. GABAergic interneurons selectively innervate different domains of pyramidal cells, thus providing the main source of feedback and feedforward inhibition (Freund and Buzsáki, 1996; Miles et al., 1996). Because of their extensive axonal arborization, they can phase the output of principal cells giving rise to coherent oscillations (McBain and Fisahn, 2001; Klausberger et al., 2003, 2004; Somogyi and Klausberger, 2005) occurring at different frequencies (Buzsáki, 2002; Whittington and Traub, 2003). Oscillatory rhythms are facilitated by the intrinsic properties of GABAergic interneurons (Maccaferri and McBain, 1996) and by their electrical coupling via gap junctions (Hestrin and Galarreta, 2005; Zsiros and Maccaferri, 2005; Minneci et al., 2007).

Oriens-lacunosum moleculare (O-LM) cells constitute a subpopulation of GABAergic interneurons containing somatostatin. They have the soma and horizontal dendrites localized in stratum oriens and the axons targeting distal dendrites of CA1 pyramidal cells in stratum-lacunosum moleculare (Lacaille et al., 1987; Ali and Thomson, 1998; Maccaferri et al., 2000; Maccaferri, 2005). These neurons participate in hippocampal theta activity *in vivo* (Buzsáki, 2002; Klausberger et al., 2003) and *in vitro* (Pike et al., 2000; Gillies et al., 2002; Hájos et al., 2004; Gloveli et al., 2005).

O-LM interneurons receive an important cholinergic innervation from the medial septum–diagonal band complex of the basal forebrain (Frotscher and Léránth, 1985) and are endowed with a variety of muscarinic acetylcholine receptors and nicotinic acetylcholine receptors (nAChRs) (Levey et al., 1995; Tribollet et al., 2004) that regulate their activity (Lawrence et al., 2006; Griguoli et al., 2009). An *in vivo* study has demonstrated a key role of cholinergic activity in amplifying theta oscillations (Lee et al., 1994), and a recent *in vitro* work has outlined the role of muscarinic receptors in enhancing spike reliability and precision to theta frequency input (Lawrence et al., 2006). Whether activation of nAChRs by nicotine affects rhythmogenesis in the hippocampus is not known. Nicotine is the major substance of tobacco, responsible for the elevated risk of cardiovascular and neurological disorders, including attention and memory deficits associated with smoking.

This study was aimed at elucidating whether activation of nAChRs by nicotine may interfere with I_h and rhythmogenesis in the hippocampus. We focused on somatostatin-expressing stratum oriens interneurons and in particular on O-LM cells, the predominant horizontal cell type in the CA1 hippocampal area (Ali and Thomson, 1998; Maccaferri, 2005), because these cells exhibit intrinsic resonance and spike transfer frequency preference in the theta range (Pike et al., 2000) and have been shown to contribute to the generation of the theta rhythm *in vivo* (Klausberger et al.,

Received May 13, 2010; revised June 9, 2010; accepted June 17, 2010.

This work was supported by Ministero Istruzione Università e Ricerca Grant PRIN 2009 (E.C.). We thank M. Dibattista and L. Lagostena for useful discussions during the preparation of this manuscript.

Correspondence should be addressed to Enrico Cherubini, Neurobiology Sector, International School for Advanced Studies, Area Science Park, 34012 Basovizza, Trieste, Italy. E-mail: cher@sissa.it.

DOI:10.1523/JNEUROSCI.2446-10.2010

 0270-6474/10/3010773-11$15.00/0

2003). To target this subpopulation, we used transgenic mice expressing enhanced green fluorescent protein (EGFP) in a subset of somatostatin-containing interneurons that mostly comprise O-LM cells in the CA1 stratum oriens (Oliva et al., 2000). Surprisingly, we found that nicotine blocked I_h by directly interfering with the channel protein responsible for this current independently of nAChR activation. The inhibitory effect of nicotine on I_h resulted in a severe impairment of the pacemaker properties of these cells.

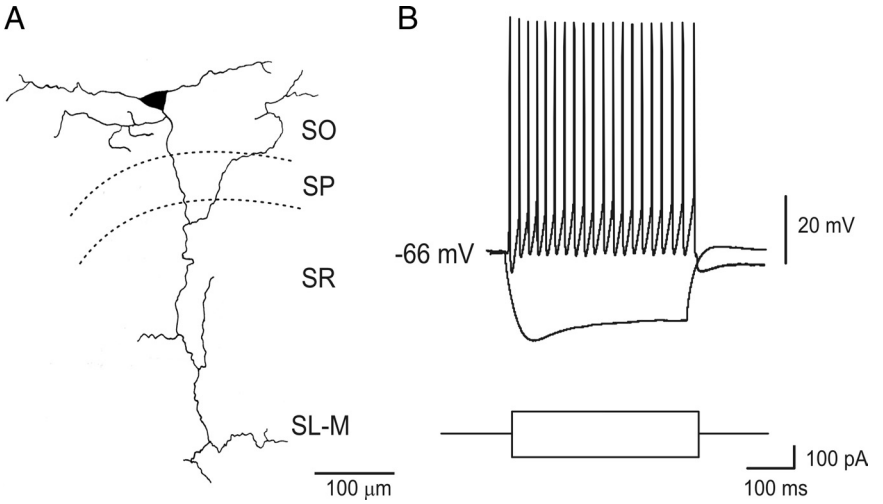

Figure 1. Identification of EGFP-positive O-LM interneurons. ***A***, *Post hoc* camera lucida reconstruction of an EGFP-positive cell recorded with patch pipette containing Neurobiotin, showing characteristic horizontal dendrites and long axon projecting to stratum-lacunosum moleculare. ***B***, Voltage responses obtained by injecting depolarizing and hyperpolarizing current steps. Note the prominent sag and the repetitive firing in the electrotonic potentials. SO, Stratum oriens; SP, stratum pyramidale; SR, stratum radiatum; SL-M, stratum-lacunosum moleculare.

Materials and Methods

Hippocampal slice preparation. All experiments were performed in accordance with the European Community Council Directive of November 24, 1986 (86/609EEC) and were approved by the local authority veterinary service. All efforts were made to minimize animal suffering and to reduce the number of animal used.

We used transgenic mice (both male and female) expressing EGFP in a subpopulation of somatostatin-containing GABAergic interneurons (GIN mice; The Jackson Laboratory) (Oliva et al., 2000; Minneci et al., 2007). To confer EGFP expression to GABAergic interneurons, an upstream regulatory sequence from the murine *Gad1* gene was used for the transgene construction (Oliva et al., 2000). Hippocampal slices were obtained from juvenile (postnatal day 14–21) using a standard protocol (Griguoli et al., 2009). Briefly, after being anesthetized with an intraperitoneal injection of urethane (2 g/kg), the brain was quickly removed from the skull and placed in ice-cold artificial CSF (ACSF) containing the following (in mM): 130 NaCl, 25 glucose, 3.5 KCl, 1.2 NaH_2PO_4, 25 $NaHCO_3$, 2 $CaCl_2$, and 1.3 $MgCl_2$ (Sigma), pH 7.3–7.4 (saturated with 95% O_2 and 5% CO_2). Transverse hippocampal slices (300 μm thick) were cut with a vibratome and stored at room temperature (22–24°C) in a holding bath containing the same solution as above. After incubation for at least 1 h, an individual slice was transferred to a submerged recording chamber and continuously superfused at 33–34°C with oxygenated ACSF at a rate of 2–3 ml/min.

Electrophysiological recordings. Whole-cell patch-clamp recordings (in current- and voltage-clamp mode) were routinely obtained from visually identified EGFP-positive cells localized in stratum oriens of the CA1 hippocampal region. We patched only those cells exhibiting round or fusiform cell bodies and horizontal dendrites, often close to the alveus border that exhibited a prominent sag in electrotonic potentials evoked by hyperpolarizing currents (Fig. 1*A*) (Zemankovics et al., 2010). Neurons were visualized using an upright fluorescent microscope (Nikon E600 FN) equipped with differential interference contrast optics and infrared video camera. Recordings were made from 166 stratum oriens EGFP-positive cells with a Multiclamp 700A amplifier (Molecular Devices) in the presence of DL-2-amino-5-phosphonopentaoic acid (DL-AP-5) (50 μM), 6,7-dinitroquinoxaline-2,3-dione (DNQX) (20 μM), and gabazine (SR 95531 hydrobromide [6-imino-3-(4-methoxyphenyl)-1(6*H*)-pyridazinebutanoic acid hydrobromide]) (10 μM) to block ionotropic glutamatergic and GABAergic synaptic currents, respectively. Patch electrodes were pulled from borosilicate glass capillaries (Hingelberg). They had a resistance of 4–6 MΩ when filled with an intracellular solution containing the following (in mM): 135 $KMeSO_4$, 10 KCl, 10 HEPES, 0.5 EGTA, 2 Na_2ATP, and 0.4 Na_2GTP, pH 7.2–7.3 with KOH (osmolarity, 280–300 mOsm). Series resistance was assessed repetitively every 5 min throughout the experiment. Series resistance values varied between 20 and 25 MΩ; cells exhibiting >15–20% changes were excluded from the analysis. Membrane potential values were corrected for a liquid junction potential of 15.1 mV.

In some experiments, the impedance (Z) amplitude profile (ZAP) was used to measure the electric resonance behavior of O-LM cells (Puil et al., 1986; Hutcheon and Yarom, 2000). The voltage response during injection through the patch pipette of a sinusoidal current (the ZAP current) with constant amplitude and linearly increasing frequency (0.5–30 Hz for 30 s; using Matlab; MathWorks) was recorded in current-clamp conditions. Resonance was manifested as a distinct and reproducible peak in the voltage response corresponding to a certain frequency. The magnitude of the ratio of the fast Fourier transform (FFT) of the voltage response to the fast Fourier transform of the ZAP stimulus formed the impedance amplitude profile. The frequency at which the impedance amplitude reached its maximum was the resonance frequency.

In current-clamp experiments, the hyperpolarization-activated current I_h gives rise to a sag in the electrotonic potentials (obtained by injecting steady hyperpolarizing currents into the cell), followed by a rebound depolarization at the end of the pulses, which often triggered action potentials. The sag was measured from the normalized steady state to peak voltage response of the cell to a hyperpolarizing current step of 250 pA (400 ms duration, from a holding potential of −70 mV) and was defined as follows: $100 \times (1 - V_{ss}/V_{peak})$, where V_{ss} is the steady-state voltage deflection from baseline, and V_{peak} is the peak voltage deflection from baseline (Narayanan and Johnston, 2007).

Currents mediated by I_h were measured in voltage-clamp conditions by applying hyperpolarizing voltage steps (2 s duration) from a holding potential of −50 mV up to −120 mV (in 10 mV increment) in the presence of tetrodotoxin (TTX) (1 μM) and cadmium (200 μM) to block fast Na^+ channels and voltage-dependent Ca^{2+} channels, respectively.

In the experiments with cadmium, NaH_2PO_4 was omitted from the bathing solution. The current–voltage (I–V) relationship was obtained by measuring the steady-state current values at the end of 2 s voltage steps after subtracting the instantaneous current at the beginning of the voltage steps. The activation curve was determined from tail current amplitudes (at the end of each hyperpolarized voltage step from −50 to −120 mV), measured after subtracting current responses obtained in the presence of nicotine and ZD 7288 (4-ethylphenylamino-1,2-dimethyl-6-methylaminopyrimidinium chloride) from their respective controls (Janigro et al., 1997). Current values at each voltage were normalized by current value obtained at −120 mV. The resulting values were plotted versus the hyperpolarization step voltages and were fitted with the following Boltzmann equation: $I/I_{MAX} = 1/\{1 + \exp[(V_{1/2} - V_m)/k]\}$, where $V_{1/2}$ is the voltage for half-maximum activation and deactivation, V_m is the pulse potential, and k is the slope factor.

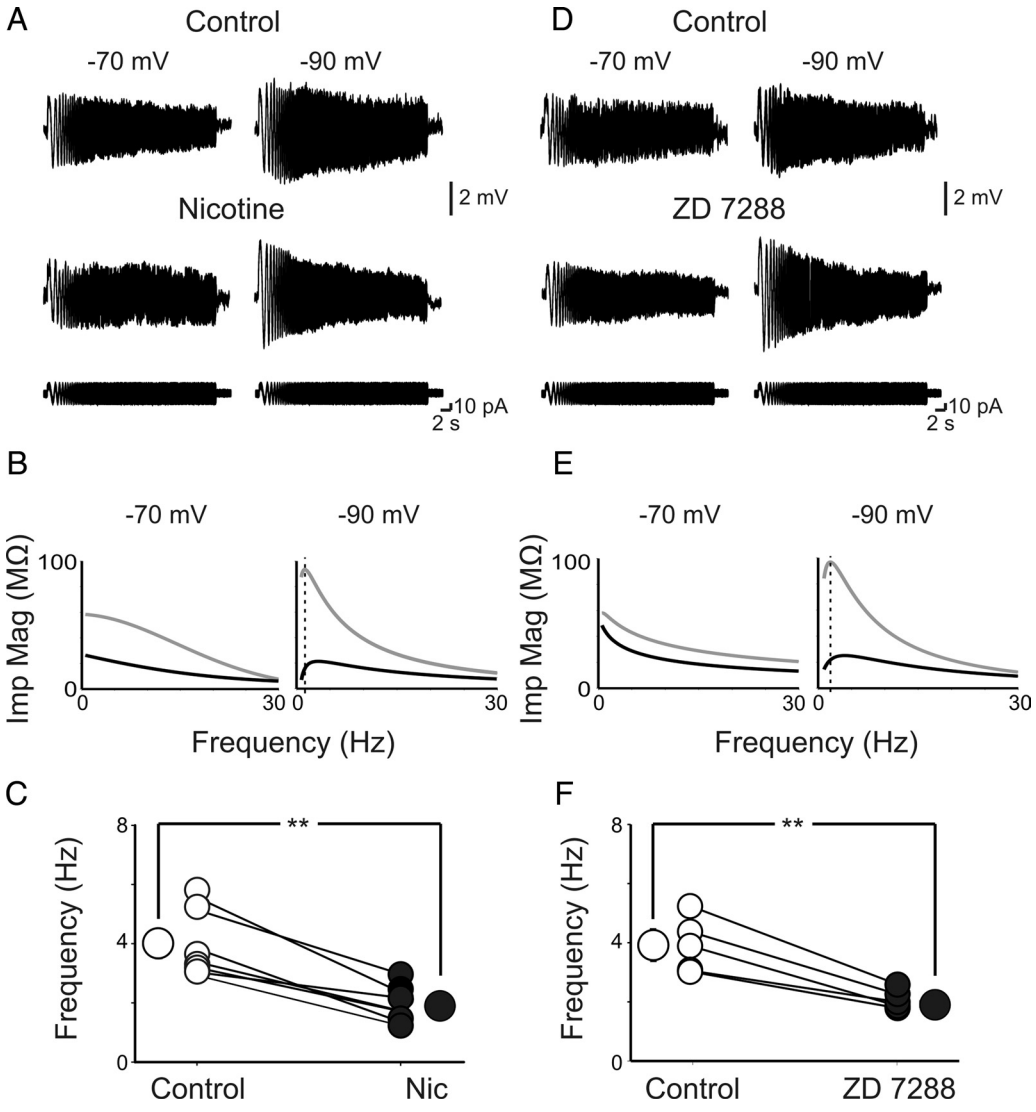

Figure 2. Nicotine affects theta resonance of O-LM interneurons. ***A***, Voltage response of an O-LM interneuron to the injection of a ZAP current at −70 mV (left) and −90 mV (right), in the absence (top traces) or presence (bottom traces) of nicotine (1 μM). Note that nicotine abolished the resonance at −90 mV but not at −70 mV. ***B***, Impedance magnitude (Imp Mag) profiles calculated from the data in ***A*** are plotted as a function of input frequencies before (black) and during (gray) nicotine application. Note the shift in the impedance magnitude peak at −90 mV (right) but not at −70 mV (left). ***C***, Each symbol represents the frequency of the impedance magnitude peak of individual cells obtained at −90 mV in control (open circles) and in the presence of nicotine (Nic; filled circles). Bigger symbols represent averaged values. Error bars are within the symbols. ***D–F***, As for ***A–C*** but in the absence or presence of ZD 7288. $^{**}p < 0.01$.

Time constants were determined by fitting currents using pClamp with a double-exponential function of the following form: $I_h(t) = A_f \exp(-t/\tau_f) + A_s \exp(-t/\tau_s)$, where $I_h(t)$ is the amplitude of the current at time t, and A_f and A_s are the initial amplitudes of the fast (τ_f) and slow (τ_s) activation time constant components, respectively.

The dose–response curve for nicotine was constructed by applying hyperpolarizing voltage steps from −50 to −120 mV in the absence or presence of the alkaloid. The amplitudes of the steady-state currents (measured at the end of the voltage steps) obtained in the presence of increasing concentrations of nicotine (from 10 nM to 10 μM) and normalized to those obtained in controls were plotted as I_h block (percentage) for different nicotine concentrations.

To investigate whether nicotine affected the intrinsic oscillatory properties of O-LM interneurons, sinusoidal currents were injected into the cells at the frequency of 4–7 Hz (in the presence of blockers of synaptic transmission) before and during application of nicotine and slopes (millivolts per millisecond) of the voltage responses during the upswing of cycle were measured.

Drugs. The following drugs were used: DL-AP-5, DNQX, SR 95531 hydrobromide, ZD 7288, forskolin, bromo-cAMP (Br-cAMP), mecamylamine, and epibatidine were all purchased from Tocris Bioscience; nicotine, dihydro-β-erytroidine (DHβE), atropine, acetylcholine, and edrophonium were purchased from Sigma; TTX was from Latoxan.

Stock solutions were made in distilled water and then aliquoted and frozen at −20°C. DNQX was dissolved in dimethylsulfoxide (DMSO). The final concentration of DMSO in the bathing solution was 0.1%. At this concentration, DMSO alone did not modify the membrane potential, input resistance, or the firing properties of O-LM interneurons. Drugs were applied in the bath via a three-way tap system, by changing the superfusion solution to one differing only in its content of drug(s). The ratio of flow rate to bath volume ensured complete exchange within 1–2 min. Nicotine was applied in the bath (for 5–7 min).

Data analysis. Data were acquired with pClamp 9.2 software (Molecular Devices) and transferred to a computer hard disk after digitization with an analog-to-digital converter (Digidata 1322; Molecular Devices). Data were digitized at 20 kHz, filtered at 2 kHz, and analyzed offline with Clampfit 9.2 (Molecular Devices). Input resistance and capacitance of the cells were measured online with the membrane test feature of the pClamp software.

Values are given as mean ± SEM. Significance of differences was assessed by Student's paired *t* test and ANOVA as indicated; $p < 0.05$ was taken as significant.

Morphology. Slices were processed for *post hoc* identification of EGFP-positive stratum oriens interneurons filled with Neurobiotin (0.2%; Vector Laboratories) during patch recordings using a standard procedure (Goldin et al., 2007; Cossart et al., 2006). Briefly, slices were fixed overnight at 4°C in a solution containing 4% paraformaldehyde in 0.1 M phosphate buffer (PB), pH 7.4. After fixation, slices were rinsed in PB, cryoprotected in sucrose (30% in PBS), and quickly frozen on dry ice. To neutralize endogenous peroxidase, slices were pretreated for 30 min in 1% H_2O_2. After several rinses in 0.01 M PBS, pH 7.4, slices were incubated for 24 h at room temperature, in 1:100 avidin–biotin peroxidase complex (Vector Laboratories) diluted in PBS containing 0.3% Triton X-100. After 30 min rinses in PBS, slices were processed with 0.04% 3–3-diaminobenzidine- HCl (Sigma) and 0.006% H_2O_2 diluted in PBS. All labeled neurons ($n = 20$) except one that was excluded from this study showed complete axonal and dendritic labeling characteristics of O-LM interneurons (McBain et al., 1994). Neurons were reconstructed using a camera lucida.

Homology model. A homology model of the pore region of HCN channels has been developed (Giorgetti et al., 2005) based on the following assumptions. (1) In the closed state, the topology of the inner pore of HCN channels is similar to that of K^+ channels. In particular, the orientation of the S5 and S6 helices is very similar to that of the corresponding helices of the K^+ KcsA and K^+ KirBac1.1 channels. Thus, we have used as templates the x-ray structure of these K^+ channels. (2) In the open state, the S6 helix is supposed to bend further than it is in the closed state. For this reason, the template of the open conformation was the x-ray structure of the MthK channel (Jiang et al., 2002). The structural models of the closed and open states turned out to be consistent with all the available electrophysiological data. Our modeling suggests that the bending amplitude of the S6 helix during gating is significantly smaller than that found in MthK channels (Jiang et al., 2002). The model has been further validated by a recent study (Cheng et al., 2007), in which the amino acids involved in the interaction between ZD 7288 and cilobradine with HCN channels has been identified.

Docking procedure. Nicotine and epibatidine were docked onto the modeled open structure of HCN channels, using the AUTODOCK 4.0 program. The parameters for the molecules were calculated using the AUTODOCK standard parameterization procedure (Morris et al., 1998). The Lamarckian Genetic Algorithm and 25 million energy evaluations per run were applied as a search method for the different docking results. The potential grid map for each atom type was calculated using a cubic box centered in the channel cavity, with a distance of 0.375 Å between grid points. For each complex, 100 docking runs were performed, resulting in a total of 300 calculations. The lowest energy conformations within the most populated clusters were used to hypothesize the location of the ligands. The cluster analyses were based on the root-mean-square deviation distance among the ligands on each run (root-mean-square deviation cutoff of 2 Å).

Results

In agreement with previous studies (Minneci et al., 2007; Griguoli et al., 2009), O-LM interneurons exhibited a mean resting membrane potential (measured in nonspontaneously active neurons) of 65 ± 0.4 mV and a mean input resistance of 326 ± 16 MΩ ($n = 166$). Some of them (122 of 166, 73%) fired spontaneously (the firing frequency ranged between 4 and 9.5 Hz). In addition, these cells exhibited different firing patterns in response to long (400 ms) depolarizing current pulses applied from holding potentials of −65 and −75 mV (Minneci et al., 2007; Griguoli et al., 2009), which were maintained with similar characteristics after blocking AMPA/kainate, NMDA, and $GABA_A$ receptors with DNQX (20 μM), DL-AP-5 (50 μM), and gabazine (10 μM), respectively. Hyperpolarizing current pulses of different amplitude revealed a sag in the electrotonic potentials, which was mediated by the time-dependent inwardly rectifying cationic current I_h (Fig. 1*B*) (Maccaferri and McBain, 1996; Minneci et al., 2007).

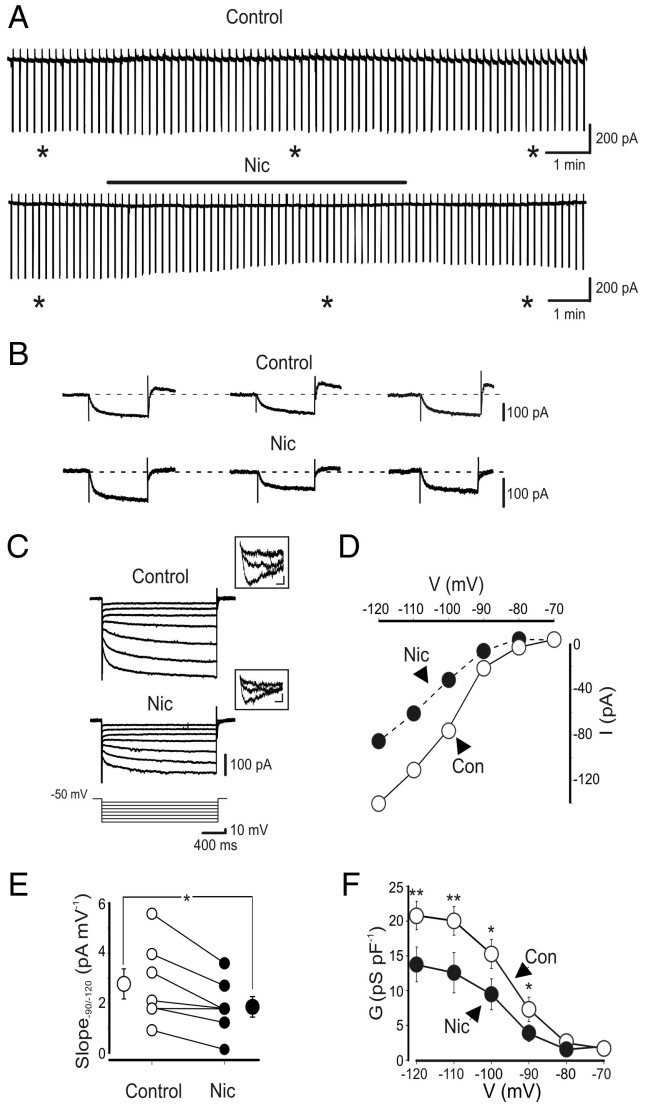

Figure 3. Nicotine reduces I_h in O-LM interneurons. ***A***, Continuous recordings of current responses evoked by hyperpolarizing voltage steps (from −60 to −120 mV, 1 s duration) repetitively delivered at 0.1 Hz, in the absence (top trace) and presence (bottom trace) of nicotine (1 μM; black bar). Note reduction of I_h amplitude with nicotine. ***B***, Leak-subtracted current responses (obtained from the traces in ***A***, asterisks) are shown in an expanded timescale. ***C***, Current responses evoked by hyperpolarizing voltage steps (10 mV increment) from a holding potential of −50 to −120 mV, in the absence (Control) or presence of nicotine (Nic) 1 μM. In the insets above the traces, tail currents evoked by voltage steps from −50 to −60, −80, and −120 mV, respectively. Calibration: 10 pA, 10 ms. ***D***, Current–voltage relationship obtained in the absence (open circles) or presence (filled circles) of nicotine for the cell shown in ***B***. Current amplitudes were measured at the end of the voltage steps. ***E***, Each symbol represents the *I–V* slope of individual cells, measured between −90 and −120 mV in the absence (open circles) or presence (filled circles) of nicotine. Bigger symbols represent averaged values. ***F***, Membrane conductances, normalized to cell capacitances, are plotted as a function of voltages in the absence (open circle) or presence (filled circles) of nicotine ($n = 6$). *$p < 0.05$, **$p < 0.01$. In this and in the following figures, vertical bars represent SEM (sometimes they are within the symbols). Con, Control.

Nicotine suppresses the theta resonance of O-LM interneurons

O-LM interneurons are known to exhibit intrinsic resonance and spike transfer frequency preferences in the theta range (Pike et al., 2000; Whittington and Traub, 2003; Gloveli et al., 2005). Reso-

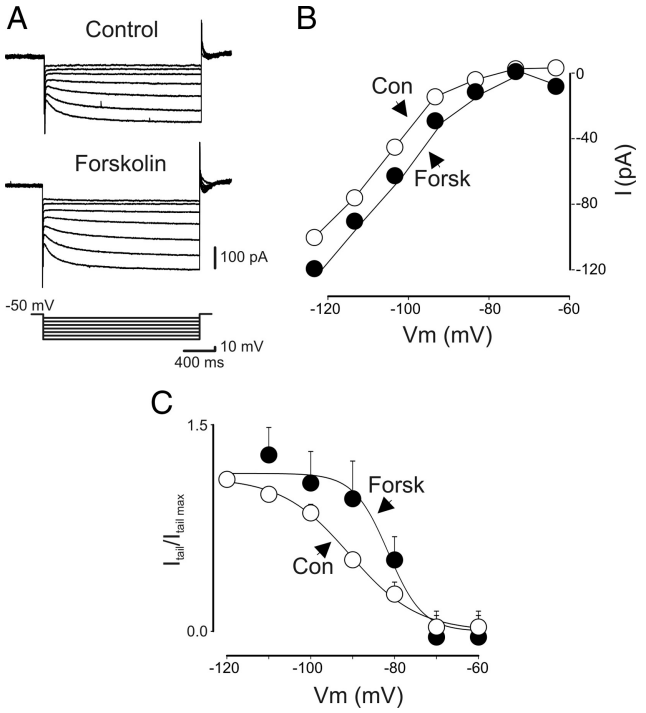

Figure 4. In a subset of O-LM interneurons, forskolin enhances I_h. ***A***, Current responses evoked by hyperpolarizing voltage steps (10 mV increments) from a holding potential of −50 to −120 mV, in the absence (Control) or presence (50 μM) of forskolin. ***B***, Current–voltage relationship obtained in the absence (open circles) or presence (filled circles) of forskolin (Forsk) for the cell shown in ***A***. ***C***, Activation curves obtained in the absence (Con) and presence of forskolin. Data points obtained from three of eight cells were fitted with the Boltzmann equation. The two curves were significantly different ($p < 0.001$, one-way ANOVA).

nance is the property by which a given neuron oscillates with maximal amplitude at certain "preferred" input frequencies (Hutcheon and Yarom, 2000). Voltage-dependent conductances underlying resonance at theta frequency are those that actively oppose changes in membrane voltages known to be mediated by Kv7/M and HCN channels, respectively. Therefore, in a first set of experiments, we have tested whether nicotine affects the subthreshold resonance behavior of O-LM interneurons. We have applied the ZAP method (Puil et al., 1986; Hutcheon and Yarom, 2000) during whole-cell current-clamp recordings. Because subthreshold resonance strictly depends on HCN channels, responsible for I_h (Hu et al., 2002), the membrane potential of the cells was manually clamped at −70 and −90 mV, respectively, by injecting a steady current through the recording electrode. As shown in the top traces of Figure 2*A*, resonance was clearly voltage dependent. Thus, a sinusoidal current with constant amplitude and linearly increasing frequency (0.5–30 Hz during 30 s; ZAP current) injected into O-LM interneurons induced a reproducible peak in the amplitude of voltage responses only at −90 mV but not at −70 mV. At this membrane potential, the impedance profile (the relationship between the voltage response and the input current as a function of the frequency) calculated by dividing the FFT of the voltage response by the FFT of input ZAP current peaked within the theta frequency range (Fig. 2*B*). Nicotine applied in the bath at the concentration of 1 μM (for 5 min) enhanced the voltage response obtained at −90 mV without significantly modifying that detected at −70 mV (Fig. 2*A*, bottom traces). The impedance magnitude increased from 22 to 97 MΩ (Fig. 2*B*). Figure 2*C* summarizes the data obtained from six cells held at −90 mV in the absence or presence of nicotine. Overall nicotine reduced the frequency of the impedance peak from 4.0 ± 0.5 to 1.8 ± 0.2 Hz ($p < 0.01$). The increase in input resistance induced by nicotine at −90 mV suggests the block of a membrane conductance active at hyperpolarized membrane potentials. To see whether I_h, which activates negative to −65 mV, was the target of nicotine action, we applied the I_h channel blocker ZD 7288 (100 μM) (Maccaferri and McBain, 1996) to the bathing solution. As shown in the bottom traces of Figure 2*D*, although ZD 7288 did not produce any significant effect at −70 mV, it almost doubled the voltage response at −90 mV. The peak of the impedance magnitude increased from 25 to 98 MΩ (Fig. 2*E*). On average, in five O-LM cells held at −90 mV, ZD 7288 reduced the frequency of the impedance magnitude peak from 4.0 ± 0.4 to 1.9 ± 0.13 Hz ($p < 0.01$) (Fig. 2*F*).

Together, these data indicate that nicotine affects resonance properties of O-LM interneurons in a way similar to ZD 7288 possibly by interfering with the slowly activating, non-inactivating inward rectifying cationic current I_h.

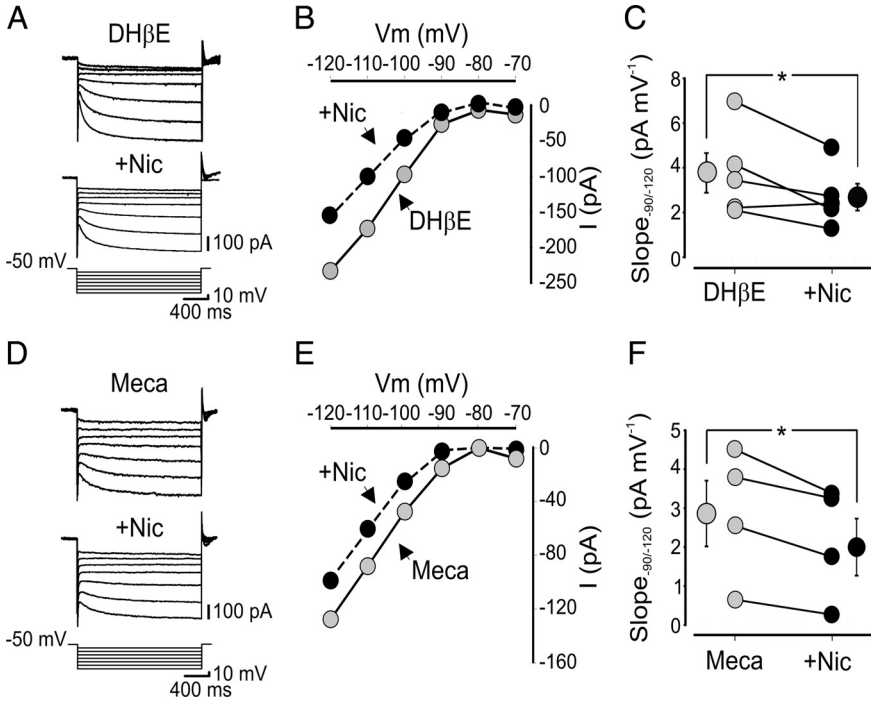

Figure 5. The effect of nicotine on I_h is independent of the activation of nAChRs. ***A***, Current responses evoked by hyperpolarizing voltage steps (10 mV increments) from a holding potential of −50 to −120 mV, in the presence of DHβE (50 μM) or DHβE plus nicotine (Nic; 1 μM). ***B***, Current–voltage relationship obtained in the presence of DHβE (gray) or DHβE plus nicotine (black) for the cell shown in ***A***. ***C***, Each symbol represents the *I–V* slope of individual cells, measured between −90 and −120 mV in the presence of DHβE and DHβE plus nicotine ($n = 5$). ***D–F***, As in ***A–C*** but in the presence of mecamylamine (Meca, 100 μM; gray) or mecamylamine plus nicotine (black). In ***C*** and ***F***, bigger symbols represent averaged values. *$p < 0.05$.

Nicotine blocks I_h by directly interfering with HCN channels

To further assess whether nicotine affects I_h, voltage-clamp experiments were performed in the presence of cadmium (200

μM) and TTX (1 μM) to block voltage-gated Ca^{2+} channels, calcium-dependent K^+ channels, and Na^+ channels, respectively. First we examined whether, in the absence of nicotine, inward currents induced by repetitive hyperpolarizing voltage steps (from −60 to −120 mV, 1 s duration, delivered at 0.1 Hz for at least 10 min) exhibited rundown. As shown in the top traces of Figure 3, *A* and *B*, current responses were stable for a prolonged period of time (>10 min). In nine O-LM cells examined, at the end of the experiments, a small nonsignificant reduction in the amplitude of I_h of 7 ± 4% ($p > 0.05$) was observed. In contrast, bath application of nicotine (1 μM, for 5–7 min) caused always a gradual reduction in amplitude of I_h (39 ± 3%; $n = 11$; $p < 0.001$). In five cells, a partial recovery of current amplitude to 78 ± 3% was observed 3–5 min after washing out nicotine ($n = 5$) (Fig. 3*A*,*B*, bottom traces). In additional experiments, hyperpolarizing voltage steps (2 s duration) of increasing amplitude (10 mV increment) were delivered to O-LM interneurons from a holding potential of −50 to −120 mV in the absence or presence of nicotine. In agreement with a previous study (Maccaferri and McBain, 1996), this protocol elicited slowly activating inward currents, followed at the end of the voltage pulses by transient tail currents (Fig. 3*C*). The current–voltage relationship revealed an inward rectifying current with a slope measured in the range −90 to −120 mV of 2.4 ± 0.3 pA/mV ($n = 16$) (Fig. 3*D*,*E*).

The activation kinetics of I_h (following a voltage step from −50 to −120 mV) was fitted with two exponentials: a fast one (τ_f) of 139 ± 10 ms ($n = 14$) and a slow one (τ_s) of 839 ± 82 ms ($n = 14$). These values were similar to those described by Maccaferri and McBain (1996).

I_h is known to be mediated by HCN channels (Biel et al., 2009) The HCN channel subunits are encoded by at least four different genes (HCN1–4, Biel et al., 2009) that are differentially distributed among cortical and subcortical structures (Robinson and Siegelbaum, 2003). Changes in homomeric and heteromeric expression of HCN subunits would determine differences in the biophysical properties of I_h as well as its sensitivity to cAMP (Pedarzani and Storm, 1995; Santoro et al., 1998; Kanyshkova et al., 2009). To assess whether native HCN channels present on O-LM interneurons contain the cAMP-sensitive subunits, hyperpolarizing voltage steps of increasing amplitude were delivered in the absence or presence of forskolin ($n = 8$), which activates adenylate cyclase, or in the presence of the long-acting cAMP derivative Br-cAMP ($n = 4$). Forskolin (50 μM) induced in three of eight cells a slight increase in amplitude of I_h (from 101 ± 27 to 116 ± 24 pA; $p < 0.05$) and a positive shift in the activation curve (Fig. 4), which reached a significant level ($p < 0.001$) (Pedarzani and Storm, 1995; Santoro et al., 1998). Br-cAMP (250 μM) (Gasparini and DiFrancesco, 1999) produced a similar effect only in one of four neurons tested (from 58 to 71 pA), suggest-

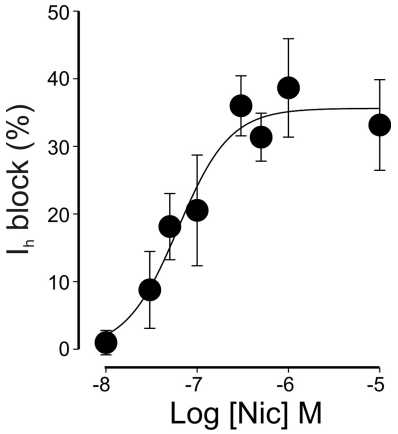

Figure 6. Nicotine reduces I_h in a concentration-dependent way. Each point represents the nicotine-induced I_h block (I_h evoked by hyperpolarizing voltage steps from −50 to −120 mV; see Materials and Methods), in the presence of increasing concentrations of nicotine (Nic) and normalized to their respective controls. Data points were fitted with the Hill equation. The EC_{50} value was 62 nM. Each point is the average of four to seven cells (total number of cells 45).

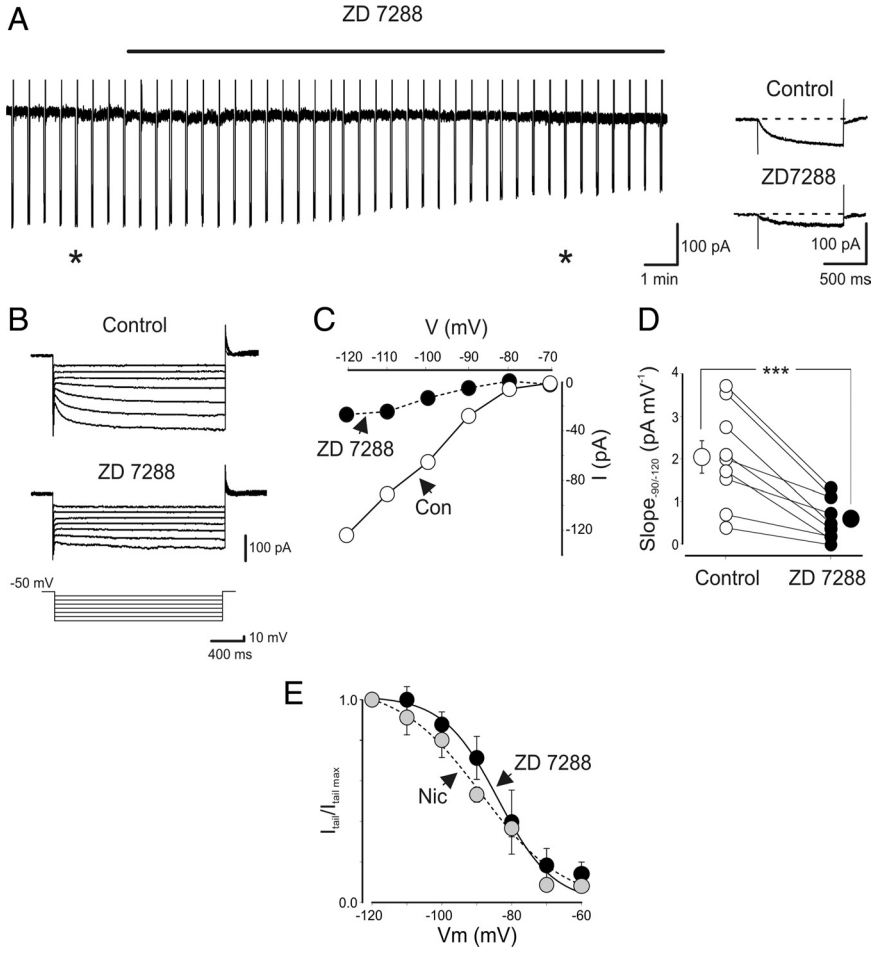

Figure 7. Nicotine reduces I_h similarly to ZD 7288. ***A***, Continuous recordings of current responses evoked by hyperpolarizing voltage steps (from −60 to −120 mV, 1 s duration) repetitively delivered at 0.1 Hz, in the absence and presence of ZD 7288 (100 μM; black bar). Individual responses obtained before and during ZD 7288 from the trace on the left (asterisks) are shown on the right with an expanded timescale. ***B***, Current responses evoked by hyperpolarizing voltage steps (10 mV increments) from a holding potential of −50 to −120 mV in the absence (Control) or presence of ZD 7288 (100 μM). ***C***, Current–voltage relationship for the cell shown in ***B***. Con, Control. ***D***, Each symbol represents *I–V* slope (measured between −90 and −120 mV) of individual cells obtained in the absence (open circles) or presence (filled circles) of ZD 7288. Bigger symbols represent averaged values. ***E***, Activation curves of nicotine-sensitive (gray circles; $n = 6$) and ZD 7288-sensitive (black circles; $n = 9$) responses obtained by subtracting tail currents recorded in the presence of nicotine (Nic) or ZD 7288 from their respective controls. ***$p < 0.001$.

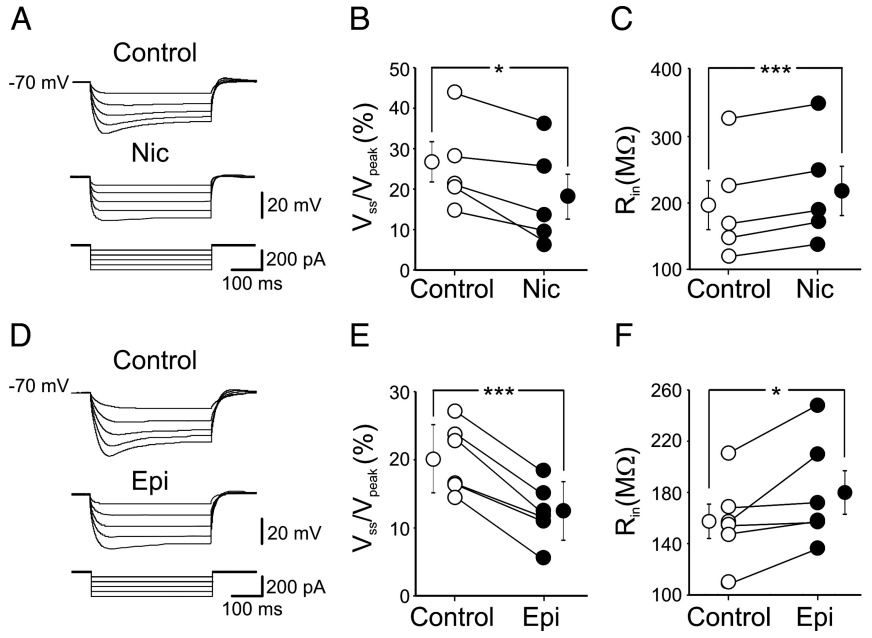

Figure 8. Epibatidine mimics the effects of nicotine on voltage sags evoked by hyperpolarizing current steps. ***A***, Voltage responses of a representative O-LM cell to injected current steps of increasing intensity (bottom) in control (top traces) or in the presence of nicotine (Nic; middle traces). ***B***, Each symbol represents the percentage ratio between the steady state and the peak values of voltage responses obtained in individual cells by hyperpolarizing current steps of 250 pA in control (open circles) or in the presence of nicotine (filled circles). ***C***, Each symbol represents the input resistance value measured in individual cells at the end of hyperpolarizing current pulses, in control (open circles) and during application of nicotine (filled circles; $n = 5$). ***D–F***, As in ***A–C*** but for epibatidine (Epi; 300 nM). Bigger symbols represent the mean ± SEM (vertical bars). $^*p < 0.05$; $^{***}p < 0.001$.

ing that, in O-LM interneurons, cAMP-sensitive HCN subunits are relatively rare.

Nicotine (applied in the bath at the concentration of 1 μM for 5 min) readily reduced I_h (Fig. 3*C*,*D*). In the −90 to −120 mV range, the slope of the current was reduced 35 ± 10% (from 2.4 ± 0.3 to 1.8 ± 0.4 pA/mV; $n = 7$; $p < 0.05$) (Fig. 3*D*,*E*).

The blocking effect of nicotine on channel conductance was more pronounced at more hyperpolarized membrane potentials. Although at −70 mV the conductance values (normalized to the cell capacitance) obtained in the absence and presence of nicotine were similar (1.8 ± 0.5 and 2.0 ± 0.4 pS/pF, respectively), at −120 mV, these were significantly different (20.9 ± 2.2 and 13.8 ± 2.7 pS/pF, respectively; $p < 0.01$) (Fig. 3*F*). Interestingly, nicotine effect on I_h was independent on nAChR activation because a similar block was observed when nicotine was applied in the presence of DHβE (50 μM) (Fig. 5*A*,*B*) or mecamylamine (100 μM) (Fig. 5*D*,*E*), known to block, at these concentrations, all nAChRs. In the presence of DHβE, nicotine induced a reduction of current slope (measured in the range −90 to −120 mV) of 27 ± 7% (from 3.8 ± 0.9 to 2.7 ± 0.6 pA/mV; $n = 5$; $p < 0.05$) (Fig. 5*B*,*C*) but in mecamylamine of 33 ± 8% (from 2.9 ± 0.8 to 2.2 ± 0.7 pA/mV; $n = 4$; $p < 0.05$) (Fig. 5*E*,*F*). These values were not significantly different from those obtained when nicotine was applied in the absence of nAChR antagonists ($p > 0.05$). It should be stressed that, in the absence of nicotine, DHβE or mecamylamine per se did not affect I_h.

To assess the minimal concentration at which nicotine affects I_h, a dose–response curve was constructed by applying hyperpolarizing voltage steps from −50 to −120 mV in the absence or presence of increasing concentrations of nicotine (from 10 nM to 10 μM). The value for the steady-state amplitude of I_h, normalized to control, was plotted versus different nicotine concentrations. Although at 30 nM the blocking effect on I_h was ~9% at 10 μM, it reached its maximum of 39 ± 7.3%. A saturating effect was found at the concentration of 1 μM. Fitting the experimental points (obtained from 45 cells, in 18 slices from 10 different animals) with the Hill equation gave an EC_{50} value of 62 nM and a Hill coefficient of 7.3, suggesting cooperativity (Fig. 6).

The blocking effect of nicotine on I_h was compared with that obtained with ZD 7288. In Figure 7*A*, the time course of ZD 7288 on I_h is illustrated. In agreement with a previous study on O-LM interneurons (Maccaferri and McBain, 1996), ZD 7288 at the concentration of 100 μM fully blocked I_h (Fig. 7*A–C*). ZD 7288 strongly reduced the slope of the *I–V* curve from 2.0 ± 0.4 to 0.59 ± 0.2 pA/mV ($n = 9$; $p < 0.001$) (Fig. 7*D*). The activation curves of nicotine- and ZD 7288-sensitive tail currents obtained at different voltages and normalized to maximal currents obtained at −120 mV were fitted with the Boltzmann equation. The $V_{1/2}$ values were −95.5 ± 1 and −85.8 ± 2.5 mV for nicotine ($n = 6$) and ZD 7288 ($n = 7$), respectively. These values were not significantly different ($p > 0.05$, one-way ANOVA). The corresponding slope factors (k) were 14.9 ± 2.5 and 6.8 ± 1.4 for nicotine and ZD 7288, respectively (Fig. 7*E*).

Epibatidine mimics the effect of nicotine on I_h

To assess whether nicotine effect on I_h is dependent on its chemical structure, we tested epibatidine, a nicotine analog, originally isolated from the frog skin, which binds with a high affinity to nAChRs (Badio and Daly, 1994). To this aim, in current-clamp conditions, hyperpolarizing current steps of increasing intensity (400 ms duration) were applied to O-LM interneurons held −70 mV. As shown in Figure 8*A* (top traces), at hyperpolarized membrane potentials, a slowly activating rectification, apparent as depolarizing sags in the electrotonic potential appeared. The amplitude of the rectification and its activation increased markedly with hyperpolarizing current steps. At the end of the current pulse, rebound depolarizing potentials were often detected. Bath application of nicotine (1 μM) almost halved the sag of the voltage response and the amplitude of the rebound depolarization (Fig. 8*A*, bottom traces). Summary data showing the percentage ratio between the steady-state and the peak values of voltage responses to hyperpolarizing current steps of 250 pA obtained in control and in the presence of nicotine are represented in Figure 8*B* (the mean normalized V_{ss}/V_{peak} values obtained before and during nicotine were 25 ± 5 and 18 ± 6, respectively; $n = 5$; $p < 0.05$). The nicotine-induced reduction of the normalized V_{ss}/V_{peak} was associated with a significant increase in membrane input resistance of 13 ± 2% (from 197 ± 37 MΩ in control to 219 ± 38 MΩ in the presence of nicotine; $n = 5$; $p < 0.001$) (Fig. 8*C*).

Like nicotine, epibatidine, at the concentration of 300 nM, reduced the sag of voltage responses and the rebound depolarization in a voltage-dependent way (Fig. 8*D*). The mean normalized V_{ss}/V_{peak} values obtained before and during epibatidine were 20 ± 5 and 12 ± 4, respectively; $n = 6$; $p < 0.001$) (Fig. 8*E*). The epibatidine-induced reduction of the normalized V_{ss}/V_{peak} was associated with a significant increase in membrane input resis-

tance of 17 ± 5% (from 157 ± 13 MΩ in control to 180 ± 17 MΩ in the presence of epibatidine; $n = 6$; $p < 0.05$) (Fig. 8*F*).

In contrast to nicotine and epibatidine, the endogenous ligand of nAChRs, acetylcholine (100 μM), applied in the presence of atropine (1 μM) to block muscarinic AChRs did not affect the voltage sag induced by hyperpolarizing current steps. The mean normalized V_{ss}/V_{peak} values obtained in the absence and presence of acetylcholine were 16 ± 3 and 14 ± 2, respectively ($n = 6$; $p > 0.05$; data not shown). Because in the brain acetylcholine is rapidly degraded by acetylcholinesterase, experiments were repeated in the presence of the acetylcholinesterase inhibitor edrophonium (20 μM; $n = 3$). Also in this case ACh failed to affect I_h.

Nicotine disrupts the oscillatory behavior of O-LM interneurons

As mentioned previously, a large number of O-LM interneurons (122 of 166) fire spontaneously in the range of 4–9.5 Hz. In 8 of 10 neurons, bath application of nicotine (1 μM) in the presence of the nAChR antagonists mecamylamine (100 μM) or DHβE (50 μM) and synaptic blockers caused a slowdown of the firing frequency from 6.1 ± 0.6 to 1.3 ± 0.6 Hz ($n = 8$; $p < 0.01$) (Fig. 9*A*,*B*). In five of eight neurons, nicotine completely blocked the firing and caused a strong membrane hyperpolarization (12 ± 0.1 mV; $n = 5$; $p < 0.001$) (Fig. 9*C*). Nicotine-induced depression of the firing rate was still present when the membrane potential was set back to the predrug membrane potential level via injection of a steady depolarizing current (in these conditions, the firing rate was reduced from 6.9 ± 0.7 to 3.8 ± 0.5 Hz; $n = 4$; $p < 0.05$) (Fig. 9*A*, arrow). This effect was similar to that obtained with ZD 7288 (Maccaferri and McBain, 1996). To elucidate whether nicotine-induced reduction of the firing rate involved I_h, the activation threshold for I_h was estimated by plotting peak amplitudes of nicotine-sensitive components of inward currents at various hyperpolarizing voltage steps versus membrane potentials. Data points through the linear portion of the *I–V* curve (in the range of −80/−110 mV) were fitted with a regression line (Kilb and Luhmann, 2000), which intercepted the *x*-axis at −67 mV, a value very close to the resting membrane potential of these cells (Fig. 9*D*). This suggests that, in our preparation, I_h is already active at rest and therefore can influence the spontaneous firing (Lupica et al., 2001).

In additional experiments, to evaluate whether nicotine affects the intrinsic oscillatory properties of O-LM interneurons, a subthreshold sinusoidal current at the theta frequency (4–7 Hz) was injected into the cells. The amplitude of the currents was adjusted to evoke spikes at the top of the sinusoidal wave.

Nicotine (1 μM) significantly reduced the rotation number [average spike per cycle (Lawrence et al., 2006)] from 1.37 ± 0.6 to 0.5 ± 0.3 ($n = 6$; $p < 0.05$) (Fig. 10*A*,*E*) and slowed down the interspike depolarizing slope from 0.26 ± 0.04 to 0.23 ± 0.03 mV/ms ($n = 5$; $p < 0.001$) (Fig. 10*A*,*B*,*D*) without altering the amplitude, duration, and shape of the action potentials (Fig. 10*C*). This indicates that nicotine severely alters the intrinsic oscillatory properties of O-LM cells and rhythmogenesis.

Similarly to nicotine, bath application of epibatidine (300 nM) in the presence of the nAChR antagonist DHβE (50 μM) and synaptic blockers significantly reduced the firing of O-LM interneurons from 4.4 ± 0.8 to 1 ± 0.7 Hz ($n = 5$; $p < 0.05$; data not shown).

A homology model predicts nicotine binding site within the HCN channel pore

To estimate nicotine binding site within the HCN channel, we docked the three-dimensional structures of nicotine and epibatidine (Fig. 11) inside our previously reported models of the HCN channels in their open configuration (Giorgetti et al., 2005). Although the docking of the ligands from the outer mouth of the channels did not show highly populated clusters, the docking from the inside of the cell, which is from the inner mouth of the channels, produced a set of highly populated clusters. The ones with the lower energies showed the ligands bound inside the inner cavity of the channel, in coincidence with the mid region of the S6 domain. The rings of the ligands were predominantly aligned with the axis of the central cavity of the channel (Fig. 11).

It can be therefore hypothesized that, to block the channels, both ligands should form hydrophobic interactions with the Ile432 and Ala425 residues. However, this hypothesis should be validated with point-directed mutagenesis experiments. Interestingly, the poses of the ligands are highly similar to those described recently for ZD 7288 and cilobradine (Cheng et al., 2007).

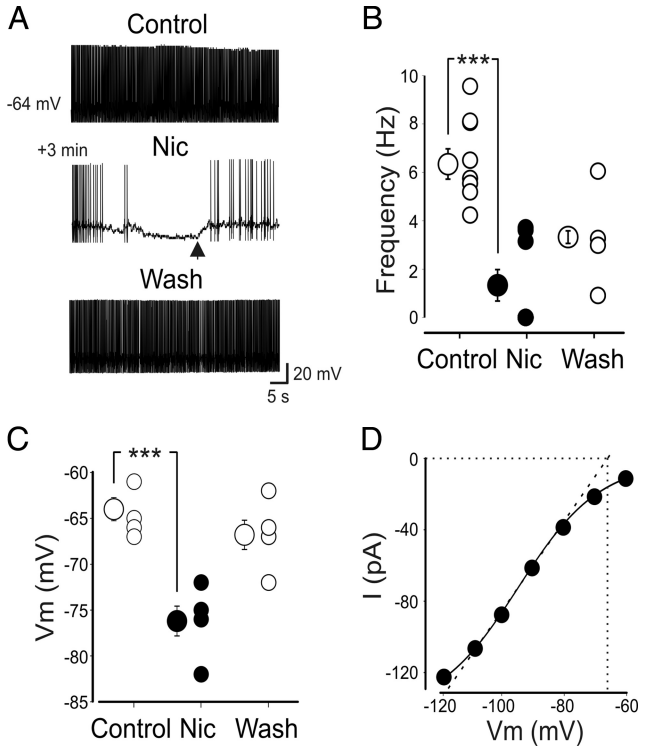

Figure 9. Nicotine reduces the spontaneous firing of O-LM cells. ***A***, Representative traces of one O-LM cell showing spontaneous firing before (Control), during (Nic; horizontal bar), and after (Wash) nicotine application. Note that the block of firing induced by nicotine was only partially restored by injecting a depolarizing steady current through the patch pipette (arrow). Full recovery was obtained 4 min after wash. ***B***, Each symbol represents the frequency value of individual cells recorded before (Control), during (Nic), and after (Wash) nicotine application. Bigger symbols represent mean values. A partial recovery was observed in five of eight cells 3–5 min after washing out nicotine. ***C***, As in ***B*** but for the resting membrane potential (V_m). ***D***, Plot of peak amplitudes of nicotine-sensitive components of inward currents at various hyperpolarizing voltage steps versus membrane potentials. Data points were fitted with the Boltzmann equation (solid line). Data points through the linear portion of the *I–V* curve (in the range of −80/−110 mV) were fitted with a regression line (dotted line) to obtain the activation threshold of I_h (*x* intercept). *$p < 0.05$; ***$p < 0.001$.

Discussion

The present data clearly show that, in O-LM interneurons, nicotine, the active component of tobacco, at a very low concentration and independently of nAChR activation, is able to reversibly reduce the time-dependent inwardly rectifying cationic current I_h responsible for the oscillatory behavior of these cells.

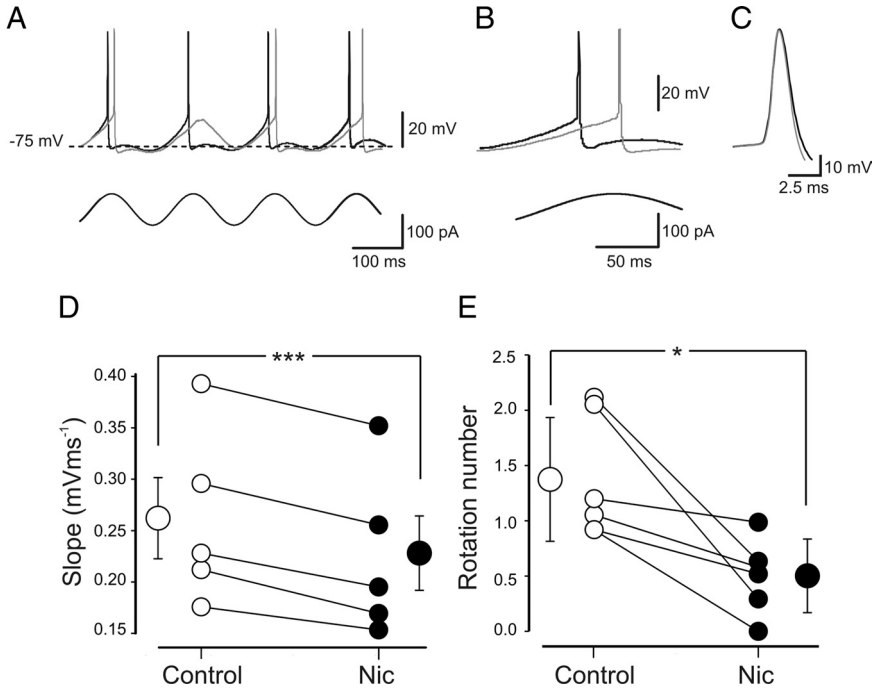

Figure 10. Nicotine slows down the depolarizing voltage slopes induced by subthreshold oscillations in the theta frequency range. ***A***, Two superimposed traces of voltage responses to injected steady subthreshold sinusoidal currents in control (black) or in the presence of nicotine (gray). Nicotine slowed down the slope and reduced the number of action potentials. ***B***, The reduction in the depolarizing voltage slope shown in ***A*** is represented on an expanded timescale. ***C***, Two action potentials from the traces in ***A*** are superimposed at a different timescale. ***D***, Each symbol represents the slope value of individual cells measured in control (open circles) or in the presence of nicotine (Nic; filled circles). ***E***, Each symbol represents the rotation number (average spikes per cycle) of individual cells obtained in control (open circles) or in the presence of nicotine (filled circles). $*p < 0.05$; $***p < 0.001$.

In a first set of experiments, using the patch-clamp technique in current-clamp mode, we have demonstrated that nicotine affects the resonance properties of O-LM interneurons. Previous work from CA1 pyramidal cells has shown the existence of two forms of slow electrical resonance occurring at the theta frequency: one at depolarizing membrane potentials (between −50 and −70 mV) dominated by I_M and the other prevailing at hyperpolarizing membrane potentials (between −70 and −95 mV) dominated by I_h (Hu et al., 2002). Blocking I_M or I_h channels with selective blockers enhanced the input resistance at their respective activation voltages and abolished the respective resonance peaks. In the present experiments from O-LM interneurons, resonance was studied only at hyperpolarizing membrane potentials in which I_h is particularly pronounced (Maccaferri and McBain, 1996). In agreement with a previous study (Pike at al. 2000), we found that O-LM interneurons optimally responded to theta inputs with maximum spiking activity occurring at input frequency at ~3–5 Hz. Surprisingly, nicotine blocked resonance at −90 mV but not at −70 mV in a way similar to ZD 7288, a selective blocker of I_h, implying that it was acting on this conductance (BoSmith et al., 1993).

In a second set of experiments, we provided direct evidence that indeed nicotine affected I_h. Similarly to ZD 7288, nicotine strongly reduced the slowly activating rectification apparent as a depolarizing sag in the electrotonic potentials evoked by hyperpolarizing current steps, further indicating that I_h was the target of this alkaloid. In voltage-clamp experiments, nicotine significantly reduced the steady-state amplitude of the currents evoked by hyperpolarizing voltage steps. The effect of nicotine on I_h did not involve activation of nAChRs because its action persisted in the presence of nAChR antagonists. Interestingly, the structurally analog of nicotine epibatidine had similar effect, whereas the physiological ligand for nAChRs, acetylcholine, was ineffective.

I_h is a mixed cationic (Na^+ and K^+) current mediated by HCN channels. Four different subunits have been so far cloned, which may assemble to form homotetramers and heterotetramers with different biophysical properties (Biel et al., 2009). In particular, the HCN2 and HCN4 subunits have been shown to confer high sensitivity to cAMP (Biel et al., 2009). The composition of native HCN channels in O-LM cells is unknown. However, the observation that both forskolin and Br-cAMP were, in the majority of cases, unable to potentiate I_h suggest that these subunits, if present, exert only a minor contribution. Alternatively, the possibility that the whole-cell condition may disrupt in some cells the cAMP-dependent regulatory pathway cannot be excluded.

The similarity of action between nicotine and ZD 7288 strongly suggest that this alkaloid blocks I_h by directly interfering with the channel protein. Molecular docking calculations have allowed estimating nicotine putative binding site within the HCN channel pore, in a position close to the one identified for ZD 7288. Based on a previous HCN channel model (Giorgetti et al., 2005) and mutagenesis experiments, Cheng et al. (2007) have found that the phenyl ring of ZD 7288 occupies a hydrophobic cavity formed by Ala425 and Ile432. The charged ring aligns with the axis of the inner pore closely corresponding to the localization of the K^+ ions, observed in the KcsA K^+ channel crystal structure. Similarly to our results, a direct interaction of nicotine with voltage-dependent K^+ channels has been described in the heart in which this alkaloid affects the shape of cardiac action potentials, independently of nAChRs activation (Greenspan et al., 1969; Pappano and Rembish, 1970; Carryl et al., 1992; Satoh H., 1997), thus contributing to cardiac arrhythmias. In particular, in canine ventricular myocytes, nicotine has been shown to reduce the transient outward K^+ current I_A (Wang et al., 2000a) and the inward rectifier potassium current mediated by Kir channels, which in cardiac cells contribute to stabilize the resting membrane potential at relatively negative values and to regulate cell excitability (Wang et al., 2000b). In a previous study aimed at clarifying whether the chronic exposure of pregnant mothers to cigarette smoke affects the intrinsic membrane properties of pedunculopontine nucleus neurons in brainstem slices of the offspring, an increase of I_h was detected (Good et al., 2006). It should be stressed however that, in contrast with the present data, in pedunculopontine nucleus neurons, I_h was studied without blocking synaptic transmission and/or nAChRs. In the present experiments, the reduction of I_h by nicotine severely affected the firing properties of O-LM interneurons and their oscillatory properties. How does nicotine-induced reduction of I_h affect the firing properties of O-LM interneurons?

One likely explanation is that nicotine reduces an inward current already active at rest that exerts a tonic depolarizing action on O-LM cells. The activation threshold of −67 mV for nicotine-sensitive inward currents found in the present experiments, very close to the resting membrane potential of O-LM cells, strongly

suggests that indeed this is the case. Therefore, similarly to ZD 7288, nicotine could affect spontaneous firing of O-LM interneurons by directly interfering with I_h. This effect was independent of nicotine-induced membrane hyperpolarization, because it persisted when the membrane was repolarized to the control level. It should be stressed, however, that this conductance becomes fully activated during the afterhyperpolarization after action potential firing. Nicotine-induced firing attenuation was dependent on the slow-down of the interspike depolarizing slope, which brings the membrane potential back to threshold for action potential firing. Interestingly, these effects occurred in the absence of any change in the shape of the action potentials, indicating a selective action of nicotine on the pacemaker current I_h. O-LM interneurons are key players in the generation of the theta rhythm (Somogyi and Klausberger, 2005) and a recent study on an *in vivo* animal model of epilepsy has clearly demonstrated that reducing I_h in O-LM interneurons severely impairs rhythmogenesis in the hippocampus (Dugladze et al., 2007).

It is worth noting that, in the present experiments, nicotine affected I_h at very low concentrations. In regular smokers, the average blood concentration of nicotine is ~220 nM/L (Varanda et al., 1985; Tang et al., 1999). In addition, with an average half-life of 2–3 h, nicotine can accumulate into the blood of smokers to reach higher concentrations (Benowitz et al., 1989). The EC_{50} value for nicotine effects on I_h (~60 nM) was well below the level found in the blood of smokers and below the level necessary to block multiple K^+ currents in the heart (Tang et al., 1999; Wang et al., 2000b).

In conclusion, nicotine, by directly blocking I_h in O-LM interneurons, disrupts the temporal coding necessary for network synchronization and for generation of the theta rhythm crucial for the processing and storage of information in the brain (Buzsáki, 2002). This may be relevant for smokers.

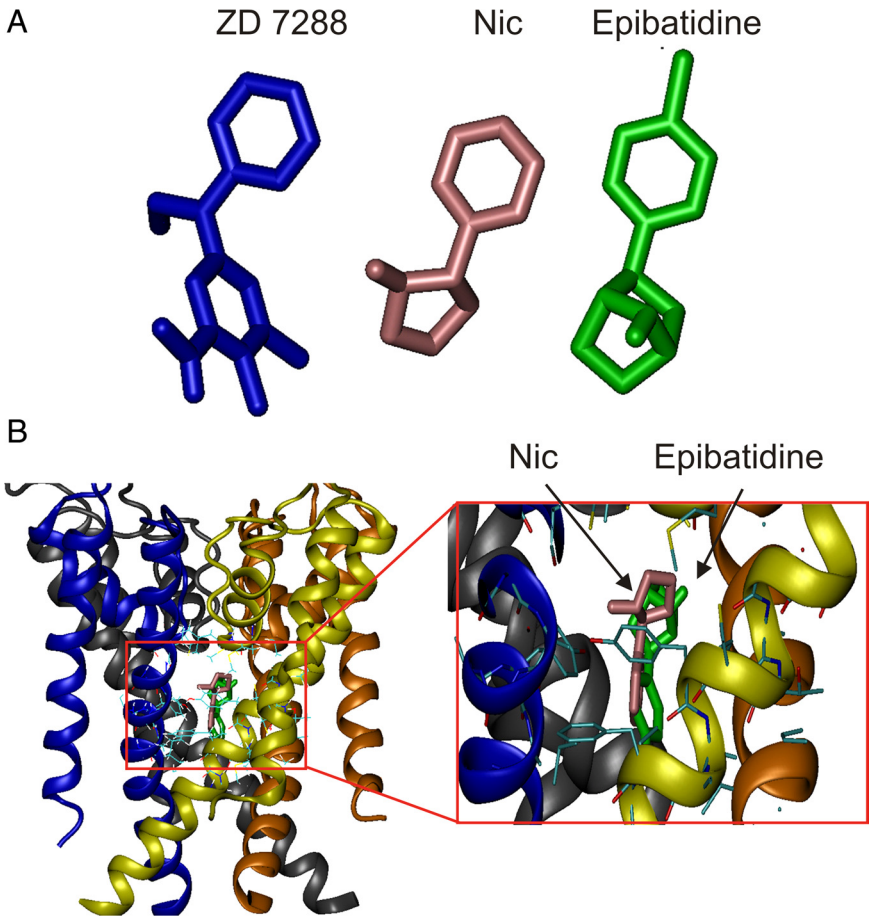

Figure 11. Putative binding site of nicotine and epibatidine into the inner pore of HCN channels. ***A***, Three-dimensional structures of ZD 7288, nicotine (Nic), and epibatidine, respectively. ***B***, Model of the tetrameric HCN channel pore structure with nicotine (pink arrow) and epibatidine (green arrow), docked in the internal cavity of the channel. Surrounding amino acids are shown in stick representation. For clarity, the four monomers are shown in different colors.

References

Ali AB, Thomson AM (1998) Facilitating pyramid to horizontal oriens-alveus interneurone inputs: dual intracellular recordings in slices of rat hippocampus. J Physiol 507:185–199.

Badio B, Daly JW (1994) Epibatidine, a potent analgetic and nicotinic agonist. Mol Pharmacol 45:563–569.

Benowitz NL, Jacob P 3rd, Yu L (1989) Daily use of smokeless tobacco: systemic effects. Ann Intern Med 111:112–116.

Biel M, Wahl-Schott C, Michalakis S, Zong X (2009) Hyperpolarization-activated cation channels: from genes to function. Physiol Rev 89:847–885.

BoSmith RE, Briggs I, Sturgess NC (1993) Inhibitory actions of ZENECA ZD 7288 on whole-cell hyperpolarization activated inward current (If) in guinea-pig dissociated sino atrial node cells. Br J Pharmacol 110:343–349.

Buzsáki G (2002) Theta oscillations in the hippocampus. Neuron 33:325–340.

Carryl OR, Gallardo-Carpentier A, Carpentier RG (1992) Effects of nicotine and ethanol on rat atrial membrane potentials. Alcohol 9:87–92.

Cheng L, Kinard K, Rajamani R, Sanguinetti MC (2007) Molecular mapping of the binding site for a blocker of hyperpolarization-activated, cyclic nucleotide-modulated pacemaker channels. J Pharmacol Exp Ther 322:931–939.

Cossart R, Petanjek Z, Dumitriu D, Hirsch JC, Ben-Ari Y, Esclapez M, Bernard C (2006) Interneurons targeting similar layers receive synaptic inputs with similar kinetics. Hippocampus 16:408–420.

Dugladze T, Vida I, Tort AB, Gross A, Otahal J, Heinemann U, Kopell NJ, Gloveli T (2007) Impaired hippocampal rhythmogenesis in a mouse model of mesial temporal lobe epilepsy. Proc Natl Acad Sci U S A 104:17530–17535.

Freund TF, Buzsáki G (1996) Interneurons of the hippocampus. Hippocampus 6:347–470.

Frotscher M, Léránth C (1985) Cholinergic innervation of the rat hippocampus as revealed by choline acetyltransferase immunocytochemistry: a combined light and electron microscopic study. J Comp Neurol 239:237–246.

Gasparini S, DiFrancesco D (1999) Action of serotonin on the hyperpolarization-activated cation current (I_h) in rat CA1 hippocampal neurons. Eur J Neurosci 11:3093–3100.

Gillies MJ, Traub RD, LeBeau FE, Davies CH, Gloveli T, Buhl EH, Whittington MA (2002) A model of atropine-resistant theta oscillations in rat hippocampal area CA1. J Physiol 543:779–793.

Giorgetti A, Carloni P, Mistrik P, Torre V (2005) A homology model of the pore region of HCN channels. Biophys J 89:932–944.

Gloveli T, Dugladze T, Saha S, Monyer H, Heinemann U, Traub RD, Whittington MA, Buhl EH (2005) Differential involvement of oriens/pyramidale interneurones in hippocampal network oscillations in vitro. J Physiol 562:131–147.

Goldin M, Epsztein J, Jorquera I, Represa A, Ben-Ari Y, Crépel V, Cossart R

(2007) Synaptic kainate receptors tune oriens-lacunosum moleculare interneurons to operate at theta frequency. J Neurosci 27:9560–9572.
Good CH, Bay KD, Buchanan RA, McKeon KA, Skinner RD, Garcia-Rill E (2006) Prenatal exposure to cigarette smoke affects the physiology of pedunculopontine nucleus (PPN) neurons in development. Neurotoxicol Teratol 28:210–219.
Greenspan K, Edmands RE, Knoebel SB, Fisch C (1969) Some effects of nicotine on cardiac automaticity, conduction, and inotropy. Arch Intern Med 123:707–712.
Griguoli M, Scuri R, Ragozzino D, Cherubini E (2009) Activation of nicotinic acetylcholine receptors enhances a slow calcium-dependent potassium conductance and reduces the firing of stratum oriens interneurons. Eur J Neurosci 30:1011–1022.
Hájos N, Pálhalmi J, Mann EO, Németh B, Paulsen O, Freund TF (2004) Spike timing of distinct types of GABAergic interneuron during hippocampal gamma oscillations *in vitro*. J Neurosci 24:9127–9137.
Hestrin S, Galarreta M (2005) Electrical synapses define networks of neocortical GABAergic neurons. Trends Neurosci 28:304–309.
Hu H, Vervaeke K, Storm JF (2002) Two forms of electrical resonance at theta frequencies, generated by M-current, h-current and persistent Na^+ current in rat hippocampal pyramidal cells. J Physiol 545:783–805.
Hutcheon B, Yarom Y (2000) Resonance, oscillation and the intrinsic frequency preferences of neurons. Trends Neurosci 23:216–222.
Janigro D, Martenson ME, Baumann TK (1997) Preferential inhibition of Ih in rat trigeminal ganglion neurons by an organic blocker. J Membr Biol 160:101–109.
Jiang Y, Lee A, Chen J, Cadene M, Chait BT, MacKinnon R (2002) Crystal structure and mechanism of a calcium-gated potassium channel. Nature 417:515–522.
Kanyshkova T, Pawlowski M, Meuth P, Dubé C, Bender RA, Brewster AL, Baumann A, Baram TZ, Pape HC, Budde T (2009) Postnatal expression pattern of HCN channel isoforms in thalamic neurons: relationship to maturation of thalamocortical oscillations. J Neurosci 29:8847–8857.
Kilb W, Luhmann HJ (2000) Characterization of a hyperpolarization-activated inward current in Cajal-Retzius cells in rat neonatal neocortex. J Neurophysiol 84:1681–1691.
Klausberger T, Magill PJ, Márton LF, Roberts JD, Cobden PM, Buzsáki G, Somogyi P (2003) Brain-state- and cell-type-specific firing of hippocampal interneurons in vivo. Nature 421:844–848.
Klausberger T, Márton LF, Baude A, Roberts JD, Magill PJ, Somogyi P (2004) Spike timing of dendrite-targeting bistratified cells during hippocampal network oscillations in vivo. Nat Neurosci 7:41–47.
Lacaille JC, Mueller AL, Kunkel DD, Schwartzkroin PA (1987) Local circuit interactions between oriens/alveus interneurons and CA1 pyramidal cells in hippocampal slices: electrophysiology and morphology. J Neurosci 7:1979–1993.
Lawrence JJ, Grinspan ZM, Statland JM, McBain CJ (2006) Muscarinic receptor activation tunes mouse stratum oriens interneurones to amplify spike reliability. J Physiol 571:555–562.
Lee MG, Chrobak JJ, Sik A, Wiley RG, Buzsáki G (1994) Hippocampal theta activity following selective lesion of the septal cholinergic system. Neuroscience 62:1033–1047.
Levey AI, Edmunds SM, Koliatsos V, Wiley RG, Heilman CJ (1995) Expression of m1–m4 muscarinic acetylcholine receptor proteins in rat hippocampus and regulation by cholinergic innervation. J Neurosci 15:4077–4092.
Lupica CR, Bell JA, Hoffman AF, Watson PL (2001) Contribution of the hyperpolarization-activated current I(h) to membrane potential and GABA release in hippocampal interneurons. J Neurophysiol 86:261–268.
Maccaferri G (2005) Stratum oriens horizontal interneurone diversity and hippocampal network dynamics. J Physiol 562:73–80.
Maccaferri G, McBain CJ (1996) The hyperpolarization-activated current (Ih) and its contribution to pacemaker activity in rat CA1 hippocampal stratum oriens-alveus interneurones. J Physiol 497:119–130.
Maccaferri G, Roberts JD, Szucs P, Cottingham CA, Somogyi P (2000) Cell surface domain specific postsynaptic currents evoked by identified GABAergic neurones in rat hippocampus in vitro. J Physiol 524:91–116.
McBain CJ, Fisahn A (2001) Interneurons unbound. Nat Rev Neurosci 2:11–23.
McBain CJ, DiChiara TJ, Kauer JA (1994) Activation of metabotropic glutamate receptors differentially affects two classes of hippocampal interneurons and potentiates excitatory synaptic transmission. J Neurosci 14:4433–4445.
Miles R, Tóth K, Gulyás AI, Hájos N, Freund TF (1996) Differences between somatic and dendritic inhibition in the hippocampus. Neuron 16:815–823.
Minneci F, Janahmadi M, Migliore M, Dragicevic N, Avossa D, Cherubini E (2007) Signaling properties of stratum oriens interneurons in the hippocampus of transgenic mice expressing EGFP in a subset of somatostatin-containing cells. Hippocampus 17:538–553.
Morris GM, Goodsell DS, Halliday RS, Huey R, Hart WE, Belew RK, Olson AJ (1998) Automated docking using a Lamarckian genetic algorithm and an empirical binding free energy function. J Comput Chem 19:1639–1662.
Narayanan R, Johnston D (2007) Long-term potentiation in rat hippocampal neurons is accompanied by spatially widespread changes in intrinsic oscillatory dynamics and excitability. Neuron 56:1061–1075.
Oliva AA Jr, Jiang M, Lam T, Smith KL, Swann JW (2000) Novel hippocampal interneuronal subtypes identified using transgenic mice that express green fluorescent protein in GABAergic interneurons. J Neurosci 20:3354–3368.
Pappano AJ, Rembish RA (1970) Nicotine-induced restoration of action potentials to cardiac tissue depolarized by potassium. Life Sci I 9:1381–1388.
Pedarzani P, Storm JF (1995) Protein kinase A-independent modulation of ion channels in the brain by cyclic AMP. Proc Natl Acad Sci U S A 92:11716–11720.
Pike FG, Goddard RS, Suckling JM, Ganter P, Kasthuri N, Paulsen O (2000) Distinct frequency preferences of different types of rat hippocampal neurones in response to oscillatory input currents. J Physiol 529:205–213.
Puil E, Gimbarzevsky B, Miura RM (1986) Quantification of membrane properties of trigeminal root ganglion neurons in guinea pigs. J Neurophysiol 55:995–1016.
Robinson RB, Siegelbaum SA (2003) Hyperpolarization-activated cation currents: from molecules to physiological function. Annu Rev Physiol 65:453–480.
Santoro B, Liu DT, Yao H, Bartsch D, Kandel ER, Siegelbaum SA, Tibbs GR (1998) Identification of a gene encoding a hyperpolarization-activated pacemaker channel of brain. Cell 93:717–729.
Satoh H (1997) Effects of nicotine on spontaneous activity and underlying ionic currents in rabbit sinoatrial nodal cells. Gen Pharmacol 28:39–44.
Somogyi P, Klausberger T (2005) Defined types of cortical interneurone structure space and spike timing in the hippocampus. J Physiol 562:9–26.
Tang G, Hanna ST, Wang R (1999) Effects of nicotine on K^+ channel currents in vascular smooth muscle cells from rat tail arteries. Eur J Pharmacol 364:247–254.
Tribollet E, Bertrand D, Marguerat A, Raggenbass M (2004) Comparative distribution of nicotinic receptor subtypes during development, adulthood and aging: an autoradiographic study in the rat brain. Neuroscience 124:405–420.
Varanda WA, Aracava Y, Sherby SM, VanMeter WG, Eldefrawi ME, Albuquerque EX (1985) The acetylcholine receptor of the neuromuscular junction recognizes mecamylamine as a noncompetitive antagonist. Mol Pharmacol 28:128–137.
Wang H, Shi H, Zhang L, Pourrier M, Yang B, Nattel S, Wang Z (2000a) Nicotine is a potent blocker of the cardiac A-type K^+ channels. Effects on cloned Kv4.3 channels and native transient outward current. Circulation 102:1165–1171.
Wang H, Yang B, Zhang L, Xu D, Wang Z (2000b) Direct block of inward rectifier potassium channels by nicotine. Toxicol Appl Pharmacol 164:97–101.
Whittington MA, Traub RD (2003) Interneuron diversity series: inhibitory interneurons and network oscillations in vitro. Trends Neurosci 26:676–682.
Zemankovics R, Káli S, Paulsen O, Freund TF, Hájos N (2010) Differences in subthreshold resonance of hippocampal pyramidal cells and interneurons: the role of h-current and passive membrane characteristics. J Physiol 588:2109–2132.
Zsiros V, Maccaferri G (2005) Electrical coupling between interneurons with different excitable properties in the stratum lacunosum-moleculare of the juvenile CA1 rat hippocampus. J Neurosci 25:8686–8695.